COMPARISON OF LAYOUTS FOR SHINGLED BIFACIAL PV MODULES IN TERMS OF POWER OUTPUT, CELL-TO-MODULE RATIO AND BIFACIALITY

Andrew Mondon, Nils Klasen, Esther Fokuhl, Max Mittag, Martin Heinrich, Harry Wirth
Fraunhofer Institute for Solar Energy Systems (ISE), Heidenhofstraße 2, 79110 Freiburg, Germany
andrew.mondon@ise.fraunhofer.de

ABSTRACT: This contribution analyses two different module topologies for shingled solar cells that increase module power at normal operation and under partial shading conditions. A bifacial shingled parallel string layout and a bifacial shingled matrix layout are compared in terms of module output by experiment and cell-to-module (CTM) analysis. After verification of the CTM model for modules samples (0.475 m²), a calculation for full size modules is performed. Both shingled layouts, excel in output power and $CTM_{efficiency}$ in comparison to a conventional module. The shingled modules are also compared regarding partial shading response, with the matrix layout showing superior power output in most investigated cases. Finally, the newly developed concept of "SlimLine" module fabrication is introduced, which uses structured encapsulants to simplify shingle cell placement and alignment having the potential of increased assembly speed and reliability.
Keywords: Shingled, Bifacial, Electrical Properties, Module Integration, Module Manufacturing, CTM, Shading

1 INTODUCTION

The concept of shingled solar cells is currently undergoing a renaissance. It was first introduced by Dickson *et al.* in 1960 [1]. Conventional solar cells feature busbars on the front surface, which cause shading loss. On solar cells for shingling, the busbars are positioned at the edge of the cell, which is then overlapped by a neighbouring cell; hence this inactive cell area as well as the cell interspace is overlapped by active cell area, significantly increasing the share of active area within the module [1].

This contribution compares two different module layouts (see Figure 1), which are parallel shingled strings and shingled cells in matrix layout initially named "shingle-roof patterned solar cell array" [2]. The two shingled module layouts have been manufactured in the size of 475 x 1000 mm²; subsequently they have been analysed. The modules feature bifacial shingled cells (pSPEER, p-type Shingled Passivated Emitter Edge and Rear) as previously presented by Baliozian *et al.* [3].

The modules are compared regarding power output at STC condition and power output considering bifaciality. Additionally, comparisons based on cell-to-module (CTM) [4, 5] analysis are carried out. The potential module performance is calculated for full size modules and compared to a conventional full size solar cell module.

The response to partial shading is examined for both shingled concepts by applying multiple partial shading scenarios, both with a covered module rear side and under bifacial operation.

Furthermore, we present a new shingled module manufacturing concept named "SlimLine", which is based on structured EVA foils. With this concept a fast and simple placement and alignment of shingled cells is achieved.

2 MATERIALS & METHODS

2.1 Examined module layouts

Two shingled cell module concepts are examined, i.e. parallel string layout (see Figure 1, top) and matrix layout (see Figure 1, bottom). Both shingled modules feature bifacial shingled solar cells (pSPEER) in the size of 148x22 mm²; in the matrix module also "half" pSPEER cells in the size of 78x22 mm² are implemented.

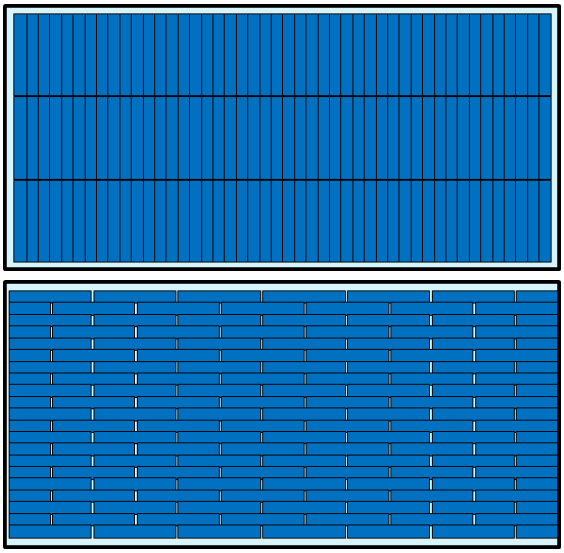

Figure 1: Schematic sketches of examined module layouts; top: parallel shingled strings layout, bottom: matrix layout

The first module (parallel string layout) comprises three strings of 46 cells each. The cells are connected in series within a string and the strings are interconnected in parallel. Since a much higher number of cells is incorporated into the module than for a standard module, substrings can be connected in parallel and only one bypass diode per module is required. The chosen orientation allows maximum module area utilisation and therefore a maximum number of incorporated cells.

The second module (matrix layout) comprises six and a half cells per row in parallel connection and 21 rows connected in series. Again the orientation was chosen for the reason of maximum module area occupancy.

The pSPEER cell's architecture corresponds to the cells presented by Baliozian *et al.* [3]. In the parallel strings setup each front side busbar of one cell is connected directly to a rear side busbar of the covering cell. In the matrix set up the shingle cells are additionally shifted along their long edge and connect two cells of the

next row. Within a cell row this results in a parallel connection of all front side busbars via the rear side busbars of the covering row of cells and vice versa. Also one half shingled cell is included into each row to achieve a rectangular cell area in shape of the module glass.

2.3 Fabrication of modules

pSPEER cells are produced at Fraunhofer ISE PV-TEC. The process is presented by Baliozian *et al.* in reference [3].

Electrically Conductive Adhesive (ECA) is printed selectively onto the busbars of the solar cells by a semi-automatic stencil printing tool. The cells are positioned by a six-axis robot at Fraunhofer ISE Module-TEC. ECA curing is performed during lamination.

In this contribution we are presenting "SlimLine" as a new manufacturing technology for simple and fast shingle module fabrication on large scale. The concept is based on the use of structured EVA foils instead of planar foils. The structure provides terraces as a guide for manual or automated positioning of cells with easy cell alignment and a well-defined shingle overlap in terms of length and height. A photo of a string, positioned on a SlimLine foil is presented in Figure 2.

Figure 2: Photo of a string before lamination, positioned on a pre-shaped "SlimLine" encapsulant foil

ECA curing is performed during module lamination. A schematic sketch of the layup cross section is shown in Figure 3.

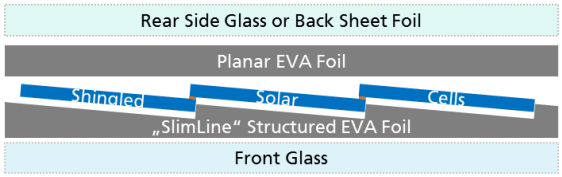

Figure 3: Schematic "SlimLine" module layup

By the use of structured EVA foils, the steps of transport of strings to the module glass, soldering, positioning of strings on the glass and interconnecting are performed in a single step.

2.2 Module efficiency analysis

We analyse the cell-to-module (CTM) ratio and the losses from module integration of each concept based on the fabricated samples of each module. We use the methodology presented by Hädrich *et al.* [4] which was extended for shingled modules [5, 6]. We perform the CTM analysis for standard testing conditions (STC) as well as for bifacial operation using the Ge-method [7] for a bifaciality of 65% and with a rear side irradiance of 10% and 20%. The used materials are characterized at Fraunhofer ISE and the resulting data is used as input for the analysis. We perform the CTM analysis regarding efficiency and module power of each concept.

The electric cell data which is used for calculations is listed in Table I, which are averaged from multiple cell measurements of the used batch of cells for the fabricated modules.

Table I: Cell data input for simulation of module outputs

Type	Area [cm²]	I_{SC} [A]	V_{OC} [V]	P_{MPP} [W]	FF [%]	η [%]
pSPEER cell	32.56	1.22	0.65	0.62	77.8	19.0
½ pSPEER	16.28	0.61	0.65	0.31	77.8	19.0

2.4 Power measurement during partial shading

Both fabricated sample modules are exposed to multiple partial shading scenarios during constant illumination in a climate chamber with integrated class B solar simulator at irradiance of approximately 1000 W/m². An illumination of the rear side of approximately 275 W/m² is achieved by means of a reflective cloth at the walls of the chamber. Shading is carried out by fixing a sheet of black cardboard in the desired shape and position directly on the front side of the module. All scenarios are considered for both, a covered and an open module rear side. The examined scenarios are graphically shown in chapter 3.4.

3 RESULTS & DISCUSSION

3.1 Measurement results on sample modules and CTM analysis

Figure 4 shows electroluminescence (EL) images of the sample modules. These show some variations in grey scale, which mainly indicates cell mismatch. The measured module outputs are listed in Table II, including results for bifacial measurements for 10% and 20% rear side irradiance, following the GE-method.

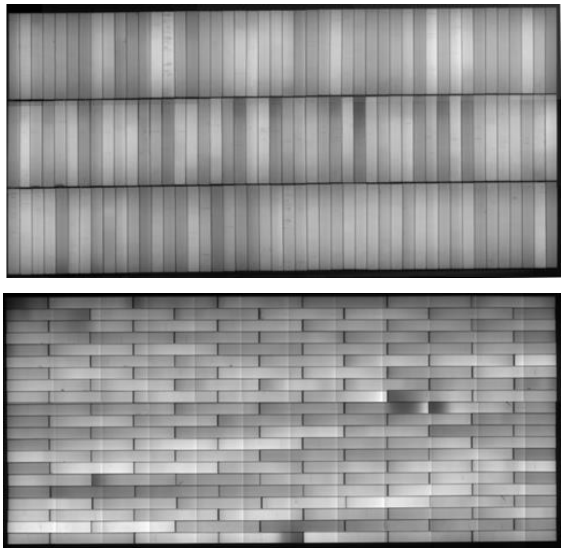

Figure 4: Electroluminescence images of the fabricated modules; top: parallel strings layout, bottom: matrix layout

Table II: Key parameters of IV measurement results of the fabricated modules at STC and with 10% and 20% additional rear side (RS) illumination

Type	I_{SC} [A]	V_{OC} [V]	P_{MPP} [W]	FF [%]
Parallel Strings	3.39	30.0	78.8	77.5
+10% RS	3.62	30.0	84.0	77.3
+20% RS	3.86	30.1	89.6	77.1
Matrix	7.30	13.6	76.2	76.9
+10% RS	7.76	13.6	81.2	76.7
+20% RS	8.21	13.7	86.2	76.6

There are 138 SPEER cells integrated into the parallel string module and only 136.5 cells in the matrix layout module. This explains the lower power output for the matrix module. Additionally, the current of the parallel string layout is lower due to a series connection of 46 cells, while in the matrix layout there are only 21 cell areas connected in series. The lower current corresponds with less resistive losses in the module, which can be observed by the increased fill factor of the parallel string layout in comparison with the matrix module.

The bifaciality calculates to 69.2% for the parallel strings module and 65.3% for the matrix module.

The calculated CTM results for power output under STC and bifacial operation are listed in Table III.

Table III: Calculacted module outputs and CTM factors for the examined module layouts, with CTM_P for power and CTM_η for efficiency and RS for rear side irradiance

Type	P_{Cells} [W]	P_{MPP} [W]	η [%]	CTM_P [%]	CTM_η [%]
Parallel-Strings	85.7	81.9	17.3	95.6	91.5
+10% RS	91.6	87.6		95.6	
+20% RS	97.5	93.4		95.6	
Matrix	84.8	80.2	17.4	94.6	91.1
+10% RS	91.2	85.4		94.6	
+20% RS	97.7	90.6		94.5	

A discrepancy between CTM calculations and the measured modules was expected due to cell mismatch, which is not included in the simulation. The relative deviance lies between 4% for the parallel layout and 5% for the matrix layout.

3.2 Full size module calculations

We have extended the CTM module calculations from the previous section for a module glass size of 1000 x 1670 mm². In this size a number of 468 cells in form of 6 strings of 78 cells may be integrated into a parallel string module. For the matrix module a number of 507 cells fit into this area in form of 6.5 cells per row and 78 rows. These calculations are compared to a conventional module with 60 solar cells. The supposed dimensions are listed in Table IV.

Table IV: Supposed module dimensions for CTM calculations on full size modules

Module type	Top & bottom margin [mm]	Side margin [mm]	String / cell spacing [mm]	Overlap [mm]
Conventional	30.7	18.5	5.4	n.a.
Parallel strings	14.75	14	15	1.25
Matrix	14.75	14	1	1.25

The CTM calculation results are listed in Table V. Here only the resulting maximum power point P_{MPP} and the power density ρ_P are given.

Table V: Calculated module outputs for full size modules

Type	P_{MPP} [W]	ρ_P [W/m²]	CTM_{Power} [%]	CTMη [%]
Convent.	270.7	162.1	97.0	83.8
+10% RS	289.0	173.1	97.2	
+20% RS	307.3	184.0	97.0	
Parallel Strings	285.2	170.8	98.1	91.3
+10% RS	305.0	182.6	98.1	
+20% RS	325.2	194.7	98.2	
Matrix	305.3	182.8	97.4	97.8
+10% RS	325.2	194.7	96.9	
+20% RS	345.1	206.6	97.0	

The power output increases in the following order: Conventional, parallel strings and matrix layout. The main cause for this increase is an increased total incorporated cell area, which is accompanied by an increased total cell power. The magnitude of CTM_{Power} ratio is similar to the conventional module, yet the $CTM_{efficiency}$ ratio is outstandingly high. Firstly, this is a result from employing more active cell area and resulting in reduced cell and string spacing. Secondly, the active cell area is further increased by covering the busbar area by active cell area. Thirdly, the reduced current from reduced cell sizes and resistance decrease from parallel connections both lead to reduced resistive losses.

3.3 Power measurement during partial shading

The investigated partial shading scenarios are shown in Figure 5. Here an electroluminescence image of the examined modules is overlain by rectangles in the shape of the desired shading areas. The shading scenarios are numbered and colour coded according to the notes below Figure 5. Scenarios 1, 2 and 3 are single shaded cells and 4, 5, 9 and 10 are two shaded cells. These were picked for reasons of fundamental comprehension. Scenarios 7 and 8 depict module coverage by leaves, dirt or similar. Scenarios 6, 11, 12, 13 and 14 were chosen to resemble systematic covering by buildings, trees and neighbouring modules. Scenario 15 resembles posts and branches.

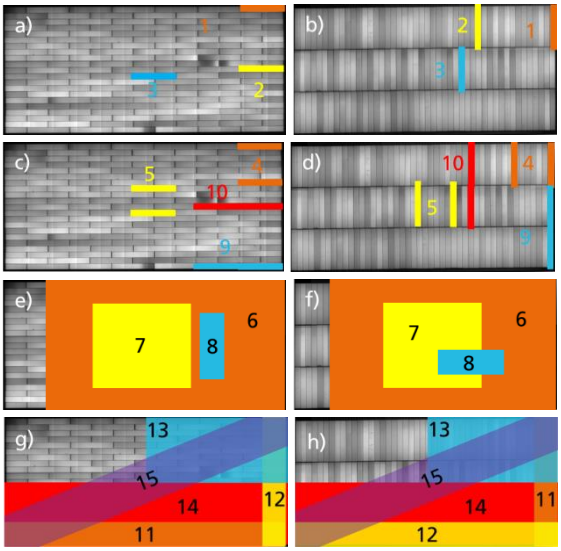

Figure 5: Partial shading scenarios; colour coding: a) & b) orange: scenario 1, yellow: scenario 2, blue: scenario 3; c) & d) orange: scenario 4, yellow: scenario 5, blue: scenario 9, red: scenario 10; e) & f) orange: scenario 6, yellow: scenario 7, blue: scenario 8; g) & h) orange: scenario 11, yellow: scenario 12, blue: scenario 13, red: scenario 14, purple: scenario 15

The resulting maximum power under partial shading is normalised to the respective initial unshaded maximum power for each scenario and plotted in Figure 6. By using normalised values, a direct comparison of power change is simplified.

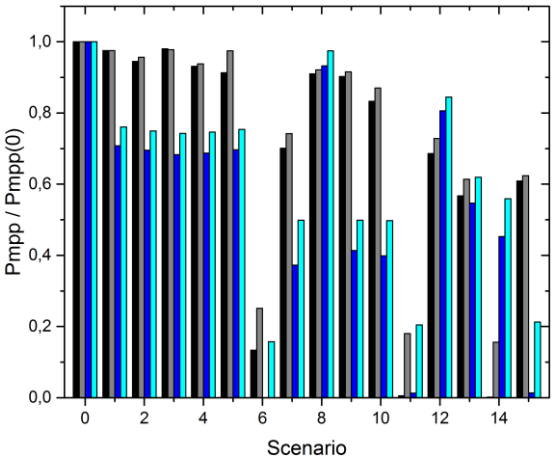

Figure 6: Maximum power at partial shading scenarios from Figure 5, normalised to unshaded case; black for the matrix module under STC, grey for the matrix module under bifacial conditions, dark blue for the parallel strings module under STC and light blue for the parallel strings module under bifacial conditions.

For most partial shading scenarios the matrix layout shows a higher power output than the parallel strings layout. Shading of a single cell leads to 33% reduction for the parallel strings layout and to a power reduction of only 2.5% for the matrix layout (scenarios 1-5). Shading of 25% of the module area leads to 63% reduction for the parallel strings layout and to a power reduction of only 30% for the matrix layout (scenario 7). Some cases were examined, in which an interruption of all series connections was planned for one module and not for the other (scenarios 6, 11, 14 and 15). To avoid performance losses, these scenarios require particular consideration when positioning these module types on the site.

With additional rear side illumination the power reduction by front side partial shading is lower in all cases within measurement uncertainty. This is mainly caused by a reduced ratio of shaded to non-shaded area and by increasing the photocurrent of the shaded cell. This applies even for scenarios which result in series connection interruption for single sided illumination cases.

4 SUMMARY & CONCLUSION

In this work we have compared two different shingled module concepts in terms of potential output power and shading behaviour and presented a new manufacturing method for shingled solar cell module fabrication (SlimLine).

The IV measurements of the module samples has demonstrated a higher output power for the parallel string layout, since more active cell area can be used for this specific configuration. The CTM calculations of both module concepts meet the measured outputs with an accuracy of 4% - 5% for both, STC and bifacial operation even though a high cell mismatch was observed.

In the case of full-size modules the occupancy by active cell area is maximized by the matrix layout. Compared to the conventional module, both examined shingled layouts show an increased power output as a result from increased active area and decreased resistive losses.

During investigation of partial shading response, we observe that the parallel strings layout performs similar to an expected shading response of a conventional layout. Less module power reduction by partial shading is observed for the matrix layout in most examined scenarios, due to the matrix of parallel and series interconnection.

In conclusion, the choice of shingled layout depends on the one hand on the number of cells of a given size which are to be incorporated into a module. On the other hand, potential shading on a site may also influence the choice of layout. Depending on the expected shading, both module layouts show increased performance under partial shading with more advantages for the matrix layout.

While a gain of 12.5 % from a full size conventional module to a matrix module was calculated, the manufacturing and cell costs of shingled modules may be increased due to usage of more wafers per module. Innovative manufacturing methods such as SlimLine may decrease total module fabrication costs by allowing very narrow cell overlap. Shingled module concepts offer main advantages in cases where highest power density and good partial shading response is beneficial, where the latter is satisfied best by the matrix layout.

ACKNOWLEGEMENTS

The authors want to thank Daniel von Kutzleben for fabrication of SlimLine foils, Michel Erlemann and Ädem Minat for ECA printing, Christoph Kutter, Gábor Horváth and Celine Hilger for robot operation, Martin Wiese and Felix Basler for lamination processes,

Alexandra Schmidt for calibrated IV measurements, Jibran Shahid for adaption of SmartClac.CTM software and Hebin Manuel and Daniel Weißer for conducting shading experiments. Also we want to thank the German Federal Ministry for Economic Affairs and Energy (BMWi) for funding the work in scope of the project PV_BAT400 under the funding code 0324145.

References

[1] D. C. [J.] Dickson, "Photovoltaic semiconductor apparartus or the like," US 2938938 A, May 31, 1960.

[2] W. Schmidt and K.-D. Rasch, "New interconnection technology for enhanced module efficiency," *IEEE Trans. Electron Devices*, vol. 37, no. 2, pp. 355–357, 1990.

[3] P. Baliozian *et al.*, "Bifacial p-type silicon shingle solar cells - the pSPEER concept," *Sol. RRL*, vol. 1700171, 2018.

[4] I. Hädrich, "Unified methodology for determining CTM ratios: Systematic prediction of module power," in *Proceedings of the 4th International Conference on Crystalline Silicon Photovoltaics*, 's-Hertogenbosch, Netherlands, 2014.

[5] M. Mittag and M. Ebert, "Systematic PV module optimization with the cell-to-module (CTM) analysis software," *Photovoltaics International*, no. 36, pp. 97–104, 2017.

[6] N. Woehrle *et al.*, "Solar cell demand for bifacial and singulated-cell module architectures," *36th Photovoltaics International*, pp. 48–62, 2017.

[7] A. Schmid, G. Duelger, G. Baarah, and U. Kraeling, "IV Measurement of Bifacial Modules: Bifacial vs. Monofacial Illumination," in *Proceedings of the 33rd European Photovoltaic Solar Energy Conference and Exhibition*, Amsterdam, 2017, pp. 1624–1627.